eJSE International

Electronic Journal of Structural Engineering 22(2) 2022

Bond strength characterization of concrete filled steel tube as structural member

Vinay Kumar Singh[1]*, Pramod Kumar Gupta[2], & S M Ali Jawaid[3]

[1,3]Department of Civil Engineering, Madan Mohan Malviya University of Technology, Gorakhpur, Uttar Pradesh, India

[2]Department of Civil Engineering, Indian Institute of Technology Roorkee, India

**Corresponding Author: vinay011990@gmail.com*

ABSTRACT: Studies done by the previous researchers in Concrete Filled Steel Tubes (CFST) have a significant focus on the bond performance of CFST. This paper includes studies on the evaluation of critical parameters such as interface condition, interface length, infilled concrete strength, and end friction and cross-section dimension in these members. It is found that the effect of interface length had very little impact on the bond stress as it shows a promising value when the interface length is in the range of 200-800 mm and after that, it gets shifted and reduced for larger interface length. But this decrease in the bond stress is affiliated with other parameters, like macro-locking, infilled concrete compressive strength distinctly affects the mean interface bond strength for the sample in the regular condition, the interface bond strength for the most part increases with infilled concrete strength. It is spotted that the friction coefficient of 0.15 is used at both column ends to provide the fixity and it becomes clear that the local buckling pattern of the stub column is independent of the end friction. In both categories of columns, the bond strength among the steel tube and infilled concrete reduced extraordinarily with increased cross-sectional dimension.

Keywords: - bond behavior, end friction, interface length, macro-locking, bond strength.

1 INTRODUCTION

In the past few decades, plentiful research had been steered to explore the bond strength between the steel tube and concrete in concrete-filled steel tubes. As these were turned out to be the extensively exercised structural elements in contemporary engineering structures. These were used as pillars in skyscrapers and multi-storey buildings, as beams in low height industrial buildings, and as arch in bridges has wide acceptance in countries like Australia, U.K., China and many other developed and developing countries in recent times. However, this practice in India is a new-fangled notion. Interestingly, CFSTs are being used as supports & beams in reinforced and unreinforced frame structures. For this sort of establishment, it should be ensured that dissimilar constituents work together and develop the composite action between them. Earlier studies revealed that continuity of strains between steel and concrete could be guaranteed if the concrete core and steel tube should be loaded simultaneously at the ends of column. Kilpatrick et. al. (1999) and Shakir-Khalil (1993) performed a series of experiments on forty samples to know effect of the interface type, shape and size of the cross-section of short CFSTs. Roeder et al. (1999) conducted the same experiments on twenty circular samples with a maximum diameter of 610 mm where eight specimens had the concrete with modest shrinkage potential and twelve had concrete with minute shrinkage. The samples had been tested at different ages varying from 20 to 60 days to know the bond characterization between steel and concrete. The foremost target of the presented manuscript is to examine the effect of critical variables like cross sectional dimension, infilled concrete strength, end friction, interface condition and interface length in concrete filled steel tube members.

2 LITERATURE SURVEY

Virdi and Dowling (1980) performed tests on numerous of steel tube filled with concrete to determine its interface mean bond strength between the infilled concrete core and the steel tube. Numerous parameters had been studied, including the concrete compressive strength, the length-diameter ratio of the interface, the diameter-thickness ratio of the tube, etc. The result of these test shows the importance of inadequacies in the manufacture of tube to contribute to full mean bond strength. It has been found that the resistance to ejection of loads in CFST is mainly due to inter-locking of infilled concrete with two types of defects. One is related to the roughness of the steel surface and other one is the

deviation in the form of the cross-section from the ideal cylindrical shape [37].

Shakir-Khalil (1993) was one among the persons who investigated the bond strength with the help of pushout tests on the sample size of 40 short concrete filled steel tubes of different cross-sections like square, circular and rectangular. The test on the specimens were carried out on some samples having block bolt of grade 4.6 as mechanical shear connector and some samples don't have the shear connectors. The steel-concrete interface length of the specimens was variable with 200, 400, 600 mm dimensions. The concrete mix was same for all the specimens throughout this experimental work. The test results of this pushout tests shows that the pushout load which is the resistance of the specimen, was depended on the shape and size of hollow steel section and on the state of interface length of the steel concrete [31,32].

Schneider (1998) conducted an experimental and analytical study on the behaviour of short columns of steel tube filled with concrete that are under compression upto failure. Samples were tested to study the influence of the shape of the steel tube and the thickness of the wall on ultimate load carrying strength of the structural member. The limitation of infilled concrete with the shape of the tube was also mentioned. The evaluated maximum resistance has been compared with the regulations in force for the construction of columns in tubular steel filled with cement. Nonlinear finite element models have been developed and verified on the basis of experimental data [30].

Giakoumelis (2004) examined the circular steel tube filled with concrete by taking numerous infilled concrete samples having different compressive strengths under axial loading. The effects of thickness of the steel tube, the rigidity of the connection between the infilled concrete and steel tube, the inclusion of the infilled concrete was examined by him. The results shows that the peak load for small reductions in deformation (approx. 3.0mm) was reached for high-strength infilled concrete, while the end load with large displacements was obtained for normal strength of infilled concrete. With increase in strength of infilled concrete, the connection between steel tube and concrete become more alarming [12].

Sakino et al., (2004) examined the behaviour of circular and square tubular column filled with concrete (CFST) for their different support conditions with a wide range of material strength through experimental work. The key parameters for the test were grade of steel such as 400, 590 or 780 MPa, the diameter, the ratio between width and thickness of steel tube and finally the compressive strength of infilled concrete such as 40, 90 MPa. The internal beam column prototypes were taken under axial load and cyclic horizontal loading with progressive increase in lateral deformation to simplify the impact of the test restrictions on performance of the member taken. The external column models were loaded laterally under variable axial load. The performance of square shaped columns exposed to a biaxial curve was also examined [29]. Ellobody et. al., (2006) studies focused on an extensive variety of infilled concrete strength and the outer diameter of the steel tube plate (D / t) thickness ratio for stub steel tubes. A precise finite element model was simulated to communicate the analysis. Precise models made of non-linear material were used for infilled concrete and steel tubes. The strength of the column and the axial load reduction curves were evaluated. The results of the finite element analysis were confirmed in relationship to the experimental results. An extensive study was done for examining the effects of different strengths of infilled concrete and cross-sectional geometries on strength and performance of circular columns with dense steel tube and infilled concrete. The column strength provided by the analysis of the finite element programme were combined with the strength of the column evaluated by using specifications provided in Euro, American and Australian codes [11].

Gupta et. al., (2007) presented, an experimental and simulated investigation of the performance of a circular column of a steel tube filled with concrete until failure loading. Wide range of samples were tested to inspect the effect of steel tube diameter and D / t ratio on the load-carrying capacity of tube columns filled with concrete. The impact of infilled concrete quality and flight volume in infilled concrete was also examined. The effect of these constraints on the delivery of the infilled concrete core was also the part of the examination. The study was validated by comparing the experimental and simulated results of the load deformation curves and the corresponding case modes. The experimental and computational investigation shows that the obtained load-carrying capacity from both the approaches was reducing with for tubular columns filled with concrete. It decreased with a certain deflection with increasing flight volume of up to 20% but increased again with 25% after output in infilled concrete [15].

Chang et. al., (2009) studied the bond performance of CFST columns with expansive infilled concrete and they found that the use of expansive infilled concrete in CFST is beneficial to refine the mean bond strength of CFST columns in short terms [10].

Oliveira et. al., (2009) experimentally examined the effect of two parameters first one was compressive strength of infilled concrete and other one was narrowness of columns. Extensive variety of circular CFST columns were tested with wide variety of infilled concrete strength and length to diameter ratio under the axial loading. A comparative studies and examination of various code gave the reasonable conclusions [39]. The ANSI and NBR showed results are lesser than results obtained by him. Still the

final load capacity was higher than predicted in ANSI code.

Aly et. al., (2010) examined 14 CFST circular column samples to find the mean bond strength behavior of composite columns that were exposed to the S.L and V.R.L procedure. The effect of infilled concrete age on the ejection strength of CFST with a diameter was examined. The age of normal strength infilled concrete was found to induce a slight decrease in ejection strength, but no steady comment could be drawn regarding high strength infilled concrete samples that could be confirmed for the small variety of infilled concrete. A comparison of column adherence obtained from current and former assessment results and existing design codes were shown. Two freshly derived mean bond strength limits were experimentally taken out and recommended for the design of structures that were mainly exposed to static or cyclic loads [3].

Tao et. al., (2011) carried out pressure tests on 64 infilled concrete filled tubular columns of infilled concrete exposed to ISO 834 fire for 90 minutes and 180 minutes, respectively. 12 unheated samples were prepared and tested for comparison, with the residual mean bond strength of CFST after exposing it with fire and the assessment results showed that mean bond strength between steel tube and infilled concrete decreased after 90 minutes of exposure fire and strength recovery was obtained upon receipt of the fire exposing time was stretched to 180 minutes. Due to the shrinkage of the infilled concrete, the mean bond strength in the CFST was found to be very delicate to its cross-sectional dimensions. Additional investigation is required for columns having large cross sections & appropriate procedures may need to be undertaken to improve mean bond strength [35].

Gupta and Singh (2014) study present a numerical examination for the performance of short Concrete filled steel tube (CFST) columns. Three-Dimensional nonlinear finite element analysis of the compression method is executed using commercial software ABAQUS v6. (2009). It is concluded that, the overall load-deflection performance and the deformed shape of the CFST column remain unchanged regardless of the end friction between the compression member and the beam (or platen) above it. Even for high end friction value of 0.5 negligible change in the result parameters was detected for short columns [17].

Qu and Chen et. al., (2015) tested 18 rectangular CFST Columns and they obtain the load v/s slip curve & the scattering of interface mean bond stress along & length of the section and around the cross-section for the numerous load stages. It has been shown that the lubrication of the steel infilled interface causes a significant reduction of the mean bond strength, and lubricating samples have mean bond strength in the range from 13.0% to 55.0% of the mean bond strength of the identical samples without lubrication. Among other parameters the compressive properties of infilled examined and cross sections of tubes have been shown to have the most important influence on the mean bond strength. Also, they suggested am empirical relation to find out the predicted value of mean ultimate bond strength for rectangular CFST by regression analysis [27].

Laboratorial exploration had been carried out on octagonal tubular stub columns made of conventional-strength steel by Godat et. al. (2012) and Zhu et. al. (2019). Their investigation presents that the residual stresses of octagonal tubular cross-sections with various plate width-to-thickness ratios could be characterized and ultimate loads of the stub columns under axial compression could also be estimated. Ultimate loads attained from laboratory experiments in in the presented work by them were also compared with those were computed on Eurocode 3 and ASCE/SEI 48 standards [EN 1993-1-1, (CEN 2005); ASCE/SEI 48-11 (ASCE 2011)] by Godat et. al., (2012) and Zhu et. al., (2019) and finally it had been concluded by these investigations that amplifying of the ultimate loads were recorded by the existing design approaches in the standards.

In accordance with Zhu et. al., (2019) and Naohiro et. al., (2017) the consideration of cross-section for Octagonal tubular cross sections have been found to have greater local buckling resistance and bond strength than rectangular tubular cross-sections [44, 25].

Studies of Tao et. al., (2016) unveiled that the effect of specimen dimension can't be overlooked. The larger the specimen size, the more substantial be the bond strength decrement. For example, after 1175 days, the bond strength of CFST with 600 mm side length was only 0.03 MPa. He also recommended that larger diameter to thickness ratio was accountable for the drop of bond strength. This conclusion was verified by various other researchers also [36].

Temperature was also observed as a crucial constraint in the examination on the bond strength. The bond strength at higher temperature and at the Frozen low temperature were also studied Song et. al., (2017), Yan et. al., (2019) and Lyu et. al., (2019). In addition, the bond strength might be affected by the curing condition of concrete, concrete strength, concrete mixture, etc. They also explored the bond behaviour in recycled aggregate concrete-filled steel tubes in laboratory. The bond strength was 0.880–1.096 MPa. Empirical formulas were projected then to predict the bond strength of specimens from other researchers, considering the influence of dimension and thickness of the steel tube. In summary, many

other parameters could affect the bond strength in different ways [34, 21, 38].

3 NUMERICAL MODELLING

3.1 *General*

To an analyst, numerical investigation of any experimental issue gives a complete opportunity to explore in detail any number of variables that may affect the concern phenomenon. Hence to simulate the CFST columns reasonably a numerous numerical models are being proposed in this work that gives the complete opportunity to explore the application and utilization of CFST columns.

A general-purpose Finite element program ABAQUS 6.14 has been used to simulate the finite element model for CFST columns. Four-nodded shell element with reduced integration & Eight-nodded brick element with three translation degree of freedom at each node were used to model the steel tube and infilled concrete core, respectively.

3.2 *Geometric Properties*

When The cross-sections taken in the modelling of the CFST has been categorized into two groups (Figure 1.), one is circular section (represented by CS) and other is square section (represented by SS).

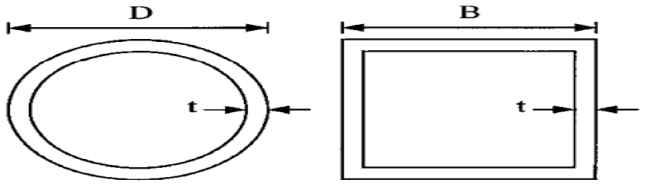

Figure 1. Cross section of Concrete Filled Steel Tubes

3.3 *Material Properties*

3.3.1 Steel Tube

An elastic-perfectly plastic behavior of steel has been modelled to simulate the specimens of steel tube. The elastic parameter such as Young's Modulus and Poisson Ratio of the material is taken as 200 kN/mm^2 and 0.3 respectively. The plastic parameters i.e., stress-strain for steel is taken in the form of true stress and true strain respectively.

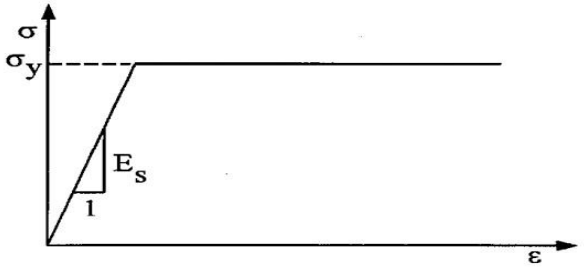

Figure 2. Elastic-perfectly plastic curve for steel.

The uniaxial behavior of steel to simulate the steel tube can be modelled by the elastic-perfectly plastic behavior of steel (Figure 2.). The response of the steel tube has been modelled by an elastic-perfectly-plastic theory with associated flow rule. When the stress points fall inside the yield surface, the behavior of the steel tube is linearly elastic. If the stresses of the steel tube reach the yield surface, the behavior of the steel tube becomes perfectly plastic. Consequently, the steel tube has been assumed to be failed and can't resist further any loading.

3.3.2 Infilled Concrete

Initial Modulus of Elasticity, E_c, of infilled concrete has been calculated as per the following equation provided in ACI,

$$E_c = 4700\sqrt{f'_{cc}} \quad \text{..... (1)}$$

Poisson's ratio for infilled concrete is taken μ=0.20, a uniaxial compressive strength and equivalent strain of unconfined infilled concrete is f'_c and ε_c respectively.

Let the uniaxial compressive strength and the corresponding strain of the unconfined infilled concrete be f'_c and ε_c respectively (Figure 3.).

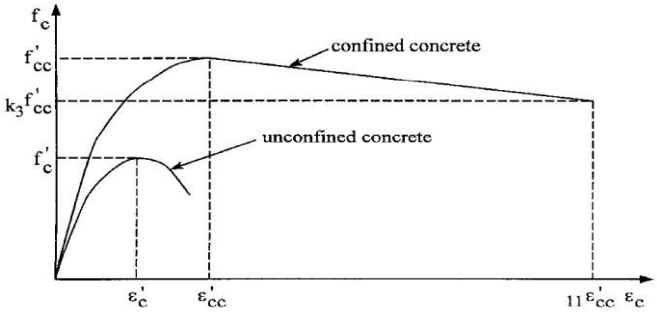

Figure 3. Equivalent uniaxial stress-strain curve for infilled concrete.

The associations between f'_{cc}, f'_c and between ε'_{cc}, ε_c is

$$f'_{cc} = f'_c + k_1 f_l \quad \text{..... (2)}$$

$$\varepsilon'_{cc} = \varepsilon'_c\left(1 + k_2 \frac{f_l}{f'_c}\right) \quad \text{..... (3)}$$

f_l is the confining stress. k_1 & k_2, are constants and they can be obtained from experimentally from the data analysis. Typical values for k_1 & k_2 can be consider with reference to the available literature as:

$k_1 = 4.1$ ..... (4)

$k_2 = 5k_1$ ..... (5)

Also, the infilled concrete is under the tri-axial stresses hence its failure should be governed by compression failure with the expanding surface on the increase in hydrostatic pressure. Hence for the plastic behaviour analysis the Linear Drucker Prager yield criteria has been deployed for the modelling of the infilled concrete.

$G = t - p\tan\beta - d = 0$ ..... (6)

Where,

$$p = \frac{(\sigma_1 + \sigma_2 + \sigma_3)}{3}$$

$$d = \left[1 - \frac{\tan\beta}{3}\right] f'_{cc}$$

$$t = \frac{\sqrt{3}J_2}{2}\left[1 + \frac{1}{K} - \left(1 - \frac{1}{K}\right)\left(\frac{r}{\sqrt{3}J_2}\right)^3\right]$$

$$r = \left[\frac{9}{2}\left(S_1^3 + S_2^3 + S_3^3\right)\right]^{\frac{1}{3}}$$

Also, S_1, S_2 *and* S_3 are principal deviatoric stresses and K and β are the constants for material parameters which can be evaluated with experimentally available data. In this analysis, 0.778, and 20^{0} are the taken values for K and β respectively.

The infilled concrete behaviour has been modelled by an elasto-plastic behaviour with the attached flow rule and the isotropic hardening rule. If plastic deformation occurs, there should be some limitation to control the expansion of the elastic area.

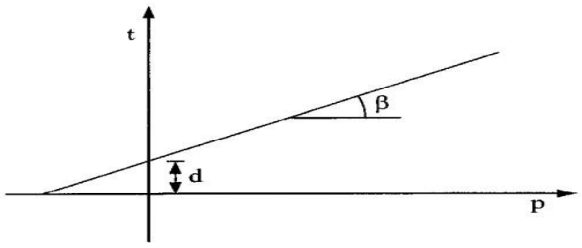

Figure 4. Linear Drucker-Prager yield criterion for infilled concrete.

Combining multidimensional stress and strain environments with a measure of measures, namely effective stress f_c and effective effort ε_c , is a commonly used approach so that all the results obtained on the stress paths can be correlated with uniaxial equivalent stress - the curve of deformation. The stress-strain relationship proposed by Saenz (1964) was widely accepted as the uniaxial stress curve for infilled concrete and has the following form

$$f_c = \frac{(E_c \epsilon_c)}{1+(R+R_E-2)\left(\frac{\epsilon_c}{\epsilon'_{cc}}\right)-(2R-1)\left(\frac{\epsilon_c}{\epsilon'_{cc}}\right)^2+R\left(\frac{\epsilon_c}{\epsilon'_{cc}}\right)^3} \quad \ldots\ldots\ldots\ldots (7)$$

Where,

$$R = \frac{R_E(R_\sigma - 1)}{(R_\epsilon - 1)^2} - \frac{1}{R_\epsilon} \quad \ldots\ldots\ldots\ldots (8)$$

And $R_\sigma = 4,\ R_\epsilon = 4$ may be used

3.4 *Interface Modelling*

To attain all the mentioned favourable advantages from the CFST columns, it is relevant that steel tube and infilled concrete core behave as a single member this makes the re-enactment of composite activity between concrete and steel. This is the most significant factor absolutely controlling the behaviour of the member. A Surface-to-Surface contact should be embraced having outer surface of infilled concrete is taken as “master surface” and inner surface of steel tube is taken as “slave surface” for proper distribution of interaction behaviour between the members. The contact surface between steel and concrete is assumed a “Hard Contact” surface and in most of the available literature, this type of surface uses a coefficient of friction value of 0.6. A hard contact surface is used to transfer the load from steel to the concrete surface. Although the range of coefficient of friction varies from 0.57 to 0.70 for steel and concrete at 0.60 the simulated specimen results show good coherence with the experimental values and this makes the axial load to be transmitted over the two surfaces simultaneously, this is the genuine contact between the two while making the surfaces separate under the influence of tensile forces.

3.5 *Meshing*

In any Finite Element based simulation, the determination of the proper element type and their size must be achieved through the computational techniques. Abaqus standard module inset in Abaqus 6.13 is utilized for modelling.

The Abaqus standard module comprises of an exhaustive element library that gives various sorts of element type and sizes with the consideration of different boundary conditions.

Mesh convergence investigations has been directed to decide ideal finite element work that provides normally precise arrangement and lower computational time. It is observed that aspect ratio of elements has very less effective on the P–ε curves if this proportion is lesser than 3.0. In this analysis the local seeding has been along the lateral direction is D/15 and along the axial direction is L/18. After the meshing, analysis has been done for refinement of node-to-node connection of different instances. A complete node-to-node intersection has been obtained by mesh refinement and, it is also very important to avoid the overlapping of instances.

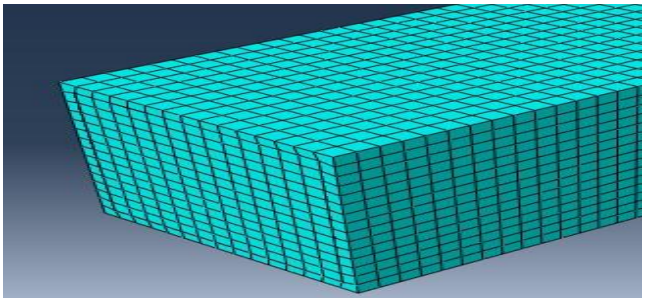

(a)

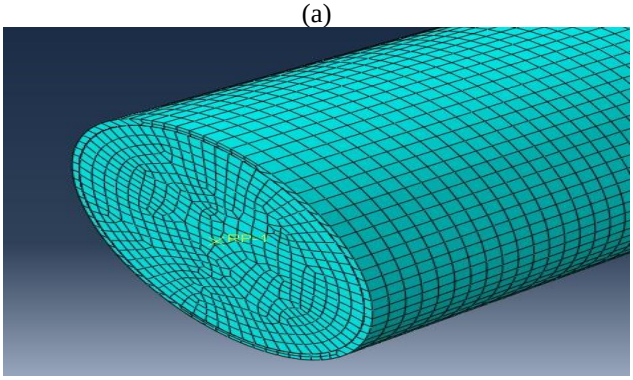

(b)

Figure 5. Finite element meshing of Concrete Filled Steel Tube.

3.6 *Loading and Boundary Conditions*

Encastre boundary condition has been taken for the bottom of CFST by seizing the displacement and rotation in U1, U2, U3 and UR1, UR2, UR3 direction respectively.

The top boundary condition of the CFST is provided by fixing displacement in x and y-directions by providing zero values to U1 & U2. Further U3 permits initial displacement in the form of applied loading which takes place in negative z-direction. UR1, UR2 and UR3 has fully restricted for initial condition, as fixity is provided at both the ends. The distribution of load is uniform over the cross-section, and it is static in general condition. After applying load in the form of initial displacement normal stress is obtained by the simulation and this normal stress value multiplied by cross sectional area of specimen will provide the load carrying capacity of the member. During the simulation, process Loading is provided by giving initial displacement at the top in negative z-direction only, the other two directions x and y having the zero initial displacements. Initial displacement for different specimens is available from the literature of respective researchers, as they had done the work experimentally. Then the results are presented by comparing load carrying capacity of the specimens. Observation of displacements has been done to carry out the load-deflection analysis of all the simulated specimen mentioned in Table-1. The ultimate displacement value is also taken from the experimental work available in literature and it is implanted in the boundary condition of the model in z-direction.

4 RESULTS AND DISCUSSIONS:

4.1 *Validation of Axial load vs Deflection*

The accuracy of the simulated model has been performed by comparing the results of the simulated models with experimental models of all the authors mentioned below in Table 1.

The experimental and simulated results for the Axial Compression vs displacement of each sample have been plotted to check the accuracy of the simulated model for the validation. Also, the corresponding ratio of ultimate load for simulated and experimental has been shown in Table 1 which can easily validate the accuracy of the simulation in terms of the loading and displacement characteristics.

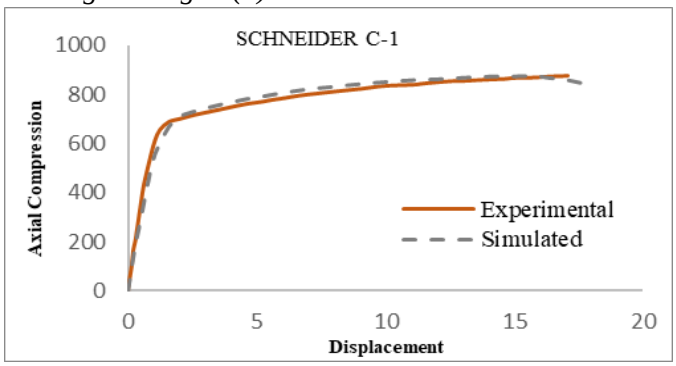

Figure 6. Axial Compression v/s Displacement curve for Experimental and Simulated model of Schneider C-1.

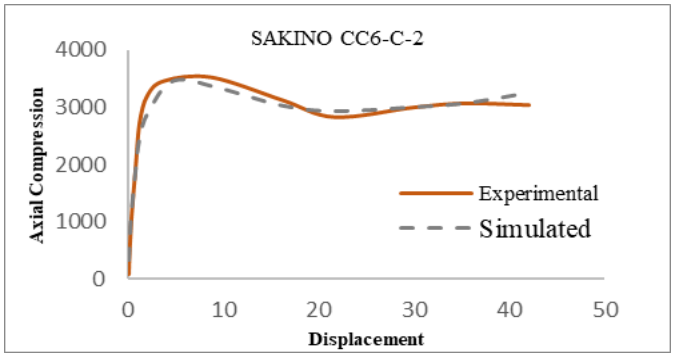

Figure 7. Axial Compression v/s Displacement curve for Experimental and Simulated model of Sakino CC6-C-2

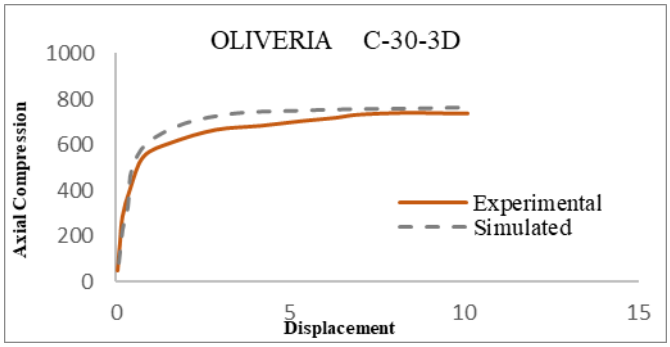

Figure 8. Axial Compression (kN) v/s Displacement (mm) curve for experimental and simulated model of Oliveira C-30-3D.

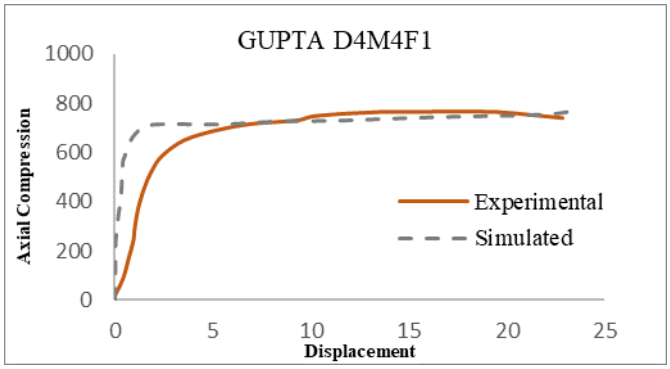

Figure 9. Axial Compression (kN) v/s Displacement (mm) curve for experimental and simulated model of Gupta D4M4F1.

Table 1. Simulated V/S Experimental load carrying capacity of various models.

Model name	Outer diameter D (mm)	Thick-ness t (mm)	Interface length L (mm)	f'_y (MPa)	f'_c (MPa)	Experi-mental load capacity N_{exp} (kN)	Simulat-ed load capacity N_{sim} (kN)	N_{sim} / N_{exp}	τ_u (N/mm)
Schneider C1 ; [4]	140.00	3.00	620.20	285.00	28.18	703.00	881.00	1.25	0.338
Schneider S1 ; [4]	127 x 127	3.15	558.80	356.00	30.45	868.00	917.00	1.06	0.327
Schneider R1 ; [4]	76 x 152	3.00	608.00	430.00	30.45	801.00	819.00	1.02	0.312
Roeder I-1 ; [6]	274.92	13.46	758.00	324.00	29.30	602.20	603.33	1.03	1.022
Roeder I-3 ; [6]	355.62	7.11	1064.00	324.00	27.90	366.00	368.20	1.06	0.032
Roeder I-3 ; [6]	609.58	11.18	1927.00	324.00	29.30	247.90	249.30	1.00	0.007
Giakoumelis C3 ; [7]	114.43	3.98	300.00	343.00	31.40	993.86	1029.43	0.97	1.026
Giakoumelis C14 ; [7]	114.54	3.84	300.00	343.00	98.90	1359.00	1425.17	1.05	1.416
Giakoumelis C8 ; [7]	115.04	4.92	300.00	365.00	104.90	1787.00	1708.66	0.96	1.724
Sakino CC6-C-2 ; [8]	239.00	4.54	717.00	507.00	25.40	3035.00	3228.00	0.94	0.624
Sakino CC6-C-8 ; [8]	238.00	4.54	714.00	507.00	77.00	5578.00	5280.00	1.06	1.029
Sakino CC6-D-2 ; [8]	361.00	4.54	1083.00	525.00	25.40	5633.00	6000.00	0.94	0.501
Ellobody S1 ; [9]	114.00	7.60	300.00	343.00	30.00	1554.20	1560.00	1.00	1.676
Ellobody S6 ; [9]	114.00	2.85	300.00	343.00	30.00	798.50	757.50	0.95	0.743
Ellobody S11 ; [9]	114.00	2.07	300.00	343.00	30.00	654.30	567.90	0.87	0.549
Ellobody S18 ; [9]	114.00	1.63	300.00	343.00	70.00	791.10	766.70	1.03	0.735
Oliveira C-30-3D ; [13]	114.30	3.35	342.90	287.33	32.70	737.00	763.40	1.04	0.659
Oliveira C-60-3D ; [13]	114.30	3.35	342.90	287.33	58.70	952.00	971.32	1.02	0.839
Oliveira C-80-3D ; [13]	114.30	3.35	342.90	287.33	88.80	1136.20	1173.62	1.03	1.013
Oliveira C-100 3D ; [13]	114.30	3.35	342.90	287.33	105.50	1453.10	1313.80	0.90	1.134
Gupta D4M3F1 ; [10]	112.56	2.89	337.68	360.00	28.88	650.00	657.97	1.01	0.581
Gupta D4M4F1 ; [10]	112.56	2.89	337.68	360.00	36.67	764.15	758.10	0.99	0.670

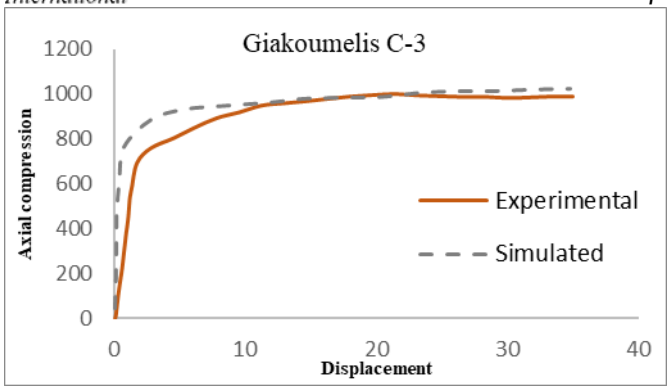

Figure 10. Axial Compression (kN) v/s Displacement (mm) curve for experimental and simulated model of Giakoumelis C-3.

From the axial compression v/s displacement curve for simulated and experimental model it can be clearly observe that the variation in the plots of simulated models over experimental models have very less deviation, and the trace of simulated curve results is as similar as the experimental curve results.

However, the variation of Ultimate load carrying capacity of simulated specimen and experimental specimen with respect to infilled concrete compressive strength and average bond stress mentioned in Table-1 is shown in Fig.12 and Fig. 13 respectively.

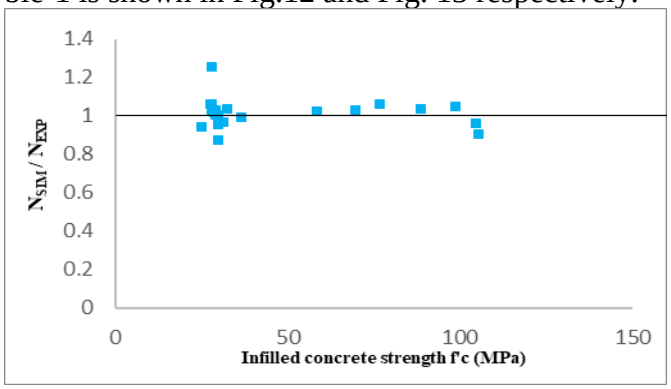

Figure 11. N_{sim} / N_{exp} v/s Infilled concrete strength f'c (MPa).

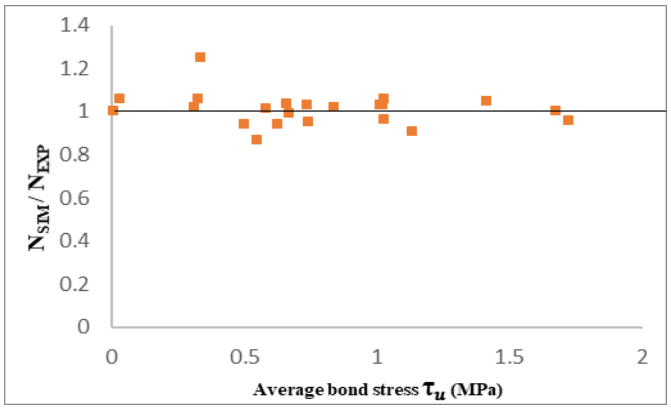

Figure 12. N_{sim} / N_{exp} v/s average bond stress τ_u (MPa).

4.2 *Interface Bond Stress*

The mean bond- stress is implemented to characterize interface bond strength. According to Eq. (9), the mean ultimate bond strength τ_u given by:

$$\tau_u = \frac{Nu}{CLi} \quad \text{..... (9)}$$

Here, Nu is ultimate load obtained from load-deflection curve, and Li is the length of the steel and infilled concrete interface, and C is the perimeter of the infilled concrete section in contact with the steel tube.[11]

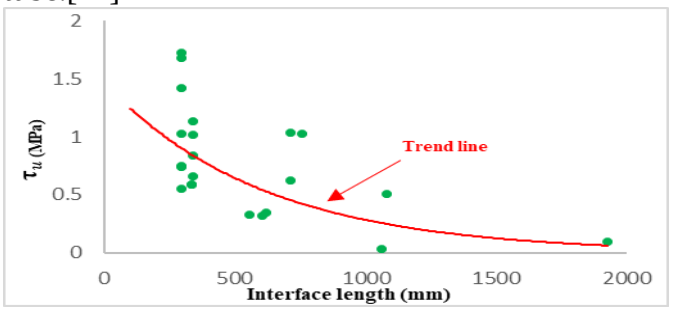

Figure 13. τu (MPa) v/s Interface length (mm) trend chart.

4.3 *Compressive Strength of Infilled Concrete*

The effect of compressive strength of infilled concrete on bond strength can be clearly seen in trend chart in Fig. 15. From the trend chart it is clear that the specimens having higher bond stress possess a high value of compressive strength as it shows a positive shift with increased strength of infilled concrete. The impact of infilled concrete strength has been investigated and tried to relate it with the cross-section segment size. Previously, it has been discussed and here also evaluated that the higher shrinkage is related to the higher grade of infilled concrete and it has progressive antagonistic impact with increased size of cross section segment.

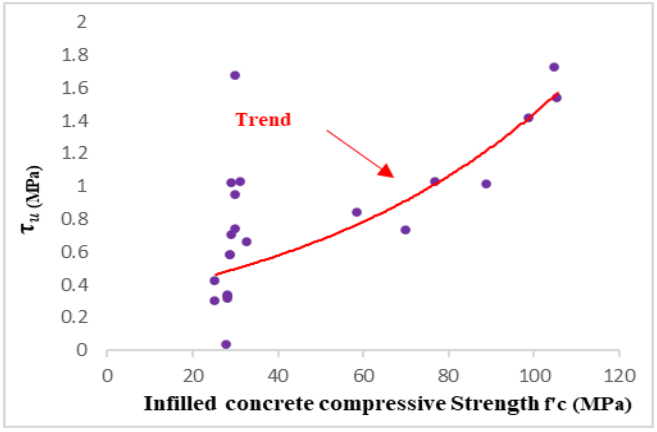

Figure 14. τ_u (MPa) v/s Infilled concrete compressive strength (MPa) trend chart.

4.4 *Bond-Slip Effect*

The bond behavior of the steel tube and infilled concrete estimated by the mean bond stress (τ), which is the axial load divided by the area of the contact edge. In this manuscript Bond slip analysis is the part of investigation on account of parameters such as infilled concrete strength and cross–section size. τ - S curve can be seen with respect to high and low strength infilled concrete and larger and small size cross-section. For infilled concrete as a parameter, τ

- S curves for high strength infilled concrete as shown in Fig. 16 shows a sharp declining slope when the value of mean bond stress is near to 1 MPa and after that it follow a normal declining slope when the value of mean bond stress is in between 0.7 and 0.1 MPa, after that is follows a second ascending slope when the value of mean bond stress is smaller than 0.7, τ-S curves for normal strength infilled concrete had a sharp declining slope when the value of mean bond stress is near to or higher than 0.6 MPa and after that it follow a normal declining slope when the value of mean bond stress is in between 0.5 and 0.6 MPa, after that is follows a second ascending slope when the value of mean bond stress is smaller than 0.5.

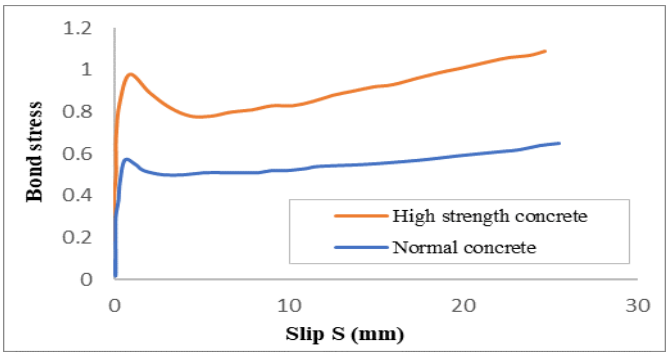

Figure 15 τ_u (MPa) v/s Slip (mm) for infilled concrete strength variation.

For cross-sectional as a parameter, τ-S curves as shown in Fig. 17 for larger size cross section had a sharp declining slope when the value of mean bond stress is near to or higher than 1.8 MPa. When the value of mean bond stress is between 1.2 & 1.7 MPa, τ-S curves generally had a decreasing slope,

τ-S curves for small size cross section had a sharp declining slope when the value of mean bond stress is near to or higher than 0.6 MPa. When the value of mean bond stress is in between 0.4 and 0.6 MPa, τ-S curves generally had a decreasing slope, trailed by a second mounting slope. When the value of mean bond stress is smaller than 0.4 MPa, τ-S curves often did not have any dropping branch.

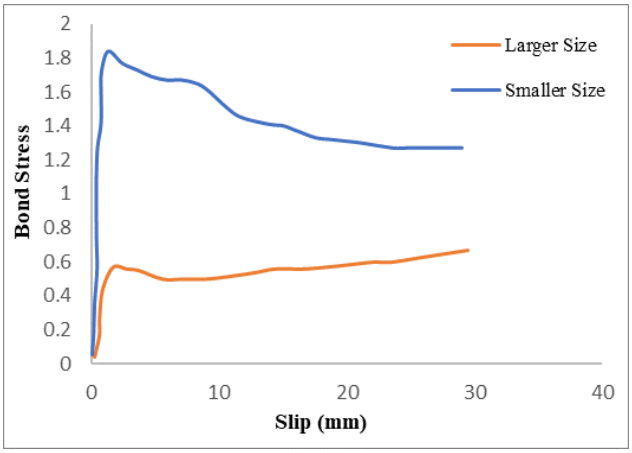

Figure 16. τ_u (MPa) v/s Slip (mm) for cross-section variation.

4.5 *Cross-Sectional Size Effect*

The variation of bond-stress with respect to cross-section is mentioned below in Fig. 18, it can be clearly seen, that bond - stress have a reliable value when the cross-sectional diameter is in between 100 -300 mm and after that the bond stress shows the decreasing trend for larger value of the diameter.

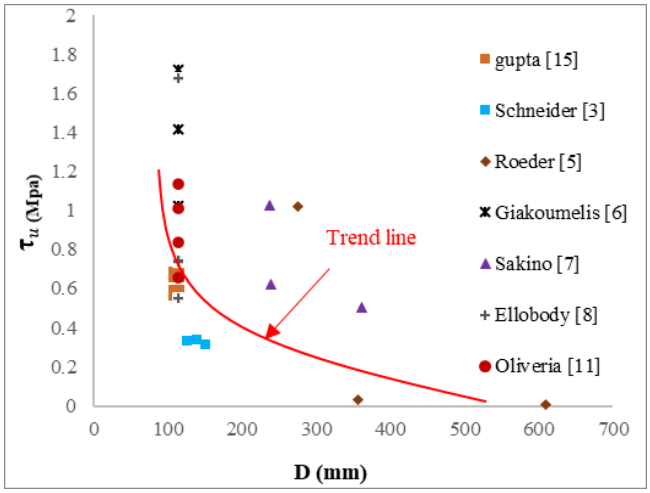

Figure 17. τ_u (MPa) v/s Diameter (mm).

Also, the variation of bond stress with respect to the D/t ratio can be seen in the Fig. 19 below it also shows a reliable value of bond stress when the D/t ratio is in the range 20-60, and for large D/t ratio the bond-stress start decreasing.

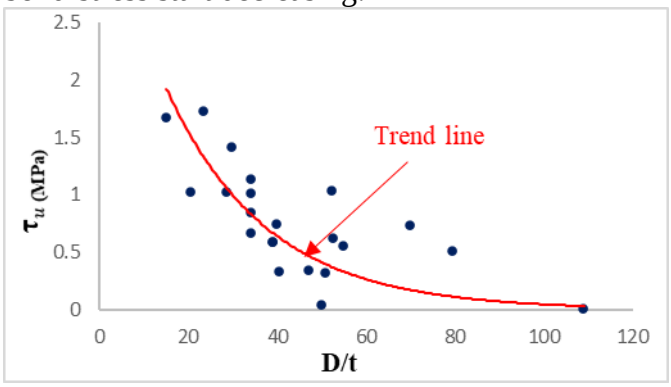

Figure 18. τu (MPa) v/s D/t

5 CONCLUSIVE REMARKS

This manuscript introduces a finite element model investigation for the simulation of concrete filled steel tubular columns loaded axially using the finite element program-based software package of ABAQUS (ABAQUS 6.13, 2009). The simulation technique endeavors to model mean bond stress of short concrete filled steel tubular columns available in literature. To judge the precision of the model, the simulated ultimate load carrying capacity and the deformed shape were compared to the corresponding values from the literature. It is revealed that the proposed model can be used to forecast the axial capacity of stub steel tubular columns filled with concrete

of compressive strength up to 100 MPa. The model is also able to capture the local buckling of steel tube, it is a common mode of failure of short CFST columns. After validation, the proposed sample is used to examine the mean bond stress variation with various parameters such as interface condition, interface length, cross-sectional geometry, infilled concrete strength, end friction. Under Sections 4.2, 4.3, and 4.4 some trend lines and curves have been presented to investigate the effect of interface length, concrete compressive strength, bond-slip, and cross-sectional dimensions on the bond strength or bond stress (τ_u). are presented by equation 9 which includes interface length of steel and infilled concrete. And this interface length introduces the macro locking with the help of interface length.

After various aspects of the investigation the concluded remarks are as follows:

5.1 Effect of interface condition

• The Ultimate mean bond stress is found distinct for different interface condition, but the common Governing factor for the interface bond condition is macro locking.

• It is conveyed that the hardness of the steel tube surface should be investigated on the microscopic scale, as per the literature. It is also found that in general steel tube surface starts moving before the infilled concrete, so it is the macro locking of steel surface which has to be countered first.

• It is found that the mean bond stress can increase by providing slit ring inside the inner surface of steel tube which can be fabricated by welding ring in actual practice.

5.2 Effect of interface length

• It is observed that the interface length has no noteworthy impact on the mean bond strength, apart from this macro-locking provides some possible extended commitment for bond strength.

• Macro locking additionally introduces the interface friction because it has the fabrication tolerance related with the internal surface of the tube. Its impact is generally confined to the former phases of the loading.

5.3 Effect of infilled concrete strength

• It is noticed that the compressive strength of infilled concrete distinctly affects the mean bond stress of the samples in the normal condition.

• In general, increase in mean bond stress is associated with higher compressive strength of infilled concrete.

• For the lubricated samples the compressive strength of infilled concrete does not have any considerable impression on the mean bond stress.

5.4 Effect of Cross-sectional Geometry and Dimension

It has been observed that the astonishing decrease in mean bond stress is due to increase in the cross-sectional dimension.

5.5 Load v/s Deflection

• It can be noticed that the initial slope of the load – deformation response attained by simulated samples is greater than that its experimental counterpart.

• The displacement of in the simulated samples at yield point is about 4 to 5 mm which is approximately 25% to 35% lesser than its experimental counterparts.

6 SCOPE FOR FUTURE RESEARCH

Despite thorough investigation in the topic some of the points further need to be explored, which are now in the future scope of the topic as follows:

• Effect of interface condition requires better understanding at microscopic level through experimentally, which further needs the chemical composition studies to improve interface condition.

• Further nonlinear investigation is required to explore on the convergence criteria.

• Effect of inside stiffeners in the tube is also included in the list of further investigation.

7 REFRENCES:

[1] ABAQUS, Standard user's manual, version 6.14, 2014 Dassault Systèmes Corp.

[2] Al-Rodan, A. K., "Comparison between BS5400 and EC4 for concrete-filled steel tubular columns" Advance in Structural Engineering, Vol. 7, No. 2, 2004, pp. 159–168.

[3] Aly, T., Elchalakani, M.,Thayalan, P., and Patnaikuni I.,"Incremental collapse threshold for pushout resistance of circular concrete filled steel tubular columns", Journal of Constructional Steel Research, Vol. 66, No. 1, 2010, pp 11-18.

[4] Aoki T., Migita Y., and Fukumoto Y., "Local buckling strength of closed polygon folded section columns", Journal of Constructional Steel Research, Vol. 20, No. 4, 1991, pp 259-270.

[5] ASCE, ".Design of steel transmission pole structures", ASCE/SEI 48-11., April 2013.

[6] Bashir, M.A., Nakayama, K., Furuuchi, H., and Ueda, T., "Numerical Simulation Of Ultimate Capacity Of Steel Pile Anchorage In Concrete-Filled Steel Box Connection", Proceeding of Japan Concrete Istitute, Vol. 32, No. 2, 2010, pp 1219-1224.

[7] BS 5400-5: 2005, "Steel, concrete and composite bridges", part 5, code of practice for the design of composite bridges, 2005, London (UK).

[8] CEN, "European Committee for Standardization: 2002", Eurocode—Basis of structural design, EN 1990. Brussels, Belgium: CEN.

[9] CEN, "European Committee for Standardization: 2005", Eurocode 3: Design of steel structures—Part 1-1: General rules and rules for buildings, EN 1993-1-1. Brussels, Belgium: CEN.

[10] Chang X. , Huang, C. K. , Jiang, D. C., and Song, Y. C., " Push-out test of pre-stressing concrete filled circular steel tube columns by means of expansive cement", Construction and Building Materials, Vol. 23, No. 1, 2009, pp. 491–497.

[11] Ellobody, E., Young, B., and Lam, D., "Behaviour of normal and high strength concrete-filled compact steel tube

circular stub columns", Journal of Constructional Steel Research, Vol. 62, No. 7, 2006, pp. 706-715.

[12] Giakoumelis, G. and Lam D., "Axial capacity of circular concrete-filled tube columns", Journal of Constructional Steel Research,Vol. 60, No. 7, 2004, pp 1049-1068.

[13] Godat, A., Legeron, F., and Bazonga D., "Stability investigation of local buckling behavior of tubular polygon columns under concentric compression", Thin-Walled Structures, Vol. 53, 2012, pp 131-140.

[14] Yoshiaki, G., Ghosh, P. K., Naoki K.,"Nonlinear Finite-Element Analysis for Hysteretic Behavior of Thin-Walled Circular Steel Columns with In-Filled Concrete", Journal of Structural Engineering (ASCE), Vol. 136, No. 11, November 2010, pp 1413-1422.

[15] Gupta, P. K., Sarda, S. M. and Kumar, M. S., "Experimental and computational study of concrete filled steel tubular columns under axial loads", Journal of Constructional Steel Research, Vol. 63, No. 2, 2007, pp 182-193.

[16] Gupta, P. K., Ahuja, A. K., and Khaudhair, Z. A., "Modelling, verification and investigation of behaviour of circular CFST columns", Structuctural Concrete, Vol. 15, No. 3, September 2014, pp. 340-349.

[17] Gupta, P. K., and Singh, H., "Numerical Study of Confinement in Short Concrete Filled Steel Tube Columns" Latin American Journal of Solids and Structures Vol. 11, No. 8, 2014, pp. 1445–1462.

[18] Hajjar, J. F. and Gourley, B. C., "Representation of concrete-filled steel tube cross-section strength", Journal of Structural Engineering, Vol. 122, No. 11, November 1996, pp.1327–1336.

[19] Han, L. H. , Wang, W. H. and Yu, H. X., "Experimental behaviour of reinforced concrete (RC) beam to concrete-filled steel tubular (CFST) column frames subjected to ISO834 standard fire", Engineering Structures, Vol. 32, No. 10, 2010, pp 3130–3144.

[20] Hwang, J. Y. and Hyo G. K. , "FE Analysis of Circular CFT Columns Considering Bond-Slip Effect: A Numerical Formulation", Mechanical Sciences, Vol. 9 No. 2, 2018, pp 245–257.

[21] Yan, J. B., Xie, W., Zhang, L., and Lin, X. C., "Bond behavior of concrete-filled steel tubes at the Arctic low temperatures", Construction of Building Materials, Vol. 210, No. 20, June 2019, pp 118–131.

[22] Kent, D. C. and Park, R., "Flexural members with confined concrete", Journal of Structural Division, Vol. 97, No. 7, July 1971, pp 1696–1700.

[23] Kilpatrick, A. E., Rangan, B. V., "Influence of interfacial shear transfer on behaviour of concrete-filled steel tubular columns", ACI Structural Journal, Vol. 96, No. 4, 1999, pp 642–648.

[24] Migita, Y. and Fukumoto, Y., "Local buckling behavior of polygonal sections", Journal of Constructional Steel Research, Vol. 41, No. 2-3, February- March 1997, pp 221–233.

[25] Naohiro, W., Kikuo, I., Tadayoshi, O. and Yosuke, K., "Local buckling behavior of octagonal hollow cross-section member under axial compression or bending shear", Special Issue: Proceedings of Euro steel, Vol. 1, No.2-3, September 2017, pp 1116-1122.

[26] Nezamian, A., and Al-Mahaidi, G. P., "The effect of cyclic loading on the bond strength of concrete plugs embedded in tubular steel piles", In: Hancock et al. (Eds.), Proceedings of advances in structures conference, June 2003, pp 1125–1129.

[27] Qu, X., Chen, Z., David A. Nethercot, L. G. and Theofanous M., "Push-out tests and bond strength of rectangular CFST columns", Steel and Composite Structures, Vol. 19, No. 1, July 2015, pp 21-41

[28] Roeder, C. W., Cameron, B., Brown, C. B., "Composite action in concrete filled tubes", Journal of Structural Engineering, ASCE, Vol. 125, No. 5, 1999, pp 477–484.

[29] Sakino, K., Nakahara, H., Morino, S. and Nishiyama, I., "Behaviour of centrally loaded concrete-filled steel-tube short columns", Journal of Structural Engineering, ASCE , Vol. 130, No. 2, February 2004, pp 180–188.

[30] Schneider, S.P., Kramer, D.R. and Sarkkinen, D.L.,"The design and construction of concrete-filled steel tube column frames", Proceedings of the 13th World Conference on Earthquake Engineering, Vancouver, Canada, August 2004, Paper No. 252.

[31] Shakir-Khalil, H., "Pushout strength of concrete-filled steel hollow section tubes", Structural Engineer, Vol. 71, No. 13, July 1993, pp 230-233.

[32] Shakir-Khalil, H., "Resistance of concrete-filled steel tubes to pushout forces", Structural Engineer, Vol. 71, No. 13, July 1993, pp 240-243.

[33] Shanmugam, N. E. and Lakshmi, B.,"State of the art report on steel–concrete composite columns", Journal of constructional steel research, Vol. 57, No. 10, October 2001, pp 1041-1080.

[34] Song, T.Y., Tao, Z., Han, L. H. and Uy, B.,"Bond behavior of concrete-filled steel tubes at elevated temperatures", Journal of Structural Engineering, ASCE, Vol. 143, No.11, November 2017, pp. 04017147:1-12

[35] Tao, Z., Han, L. H., Uy, B., and Chen, X., "Post-fire bond between the steel tube and concrete in concrete-filled steel tubular columns", Journal of Constructional Steel Research,Vol. 67, No. 3, March 2011, pp 484-496.

[36] Tao, Z., Song, T. Y., Uy, B. and Han, L. H., "Bond behavior in concrete-filled steel tubes", Journal of Constructional Steel Research, Vol. 120, April 2016, pp 81-93.

[37] Virdi, K. S. and Dowling, P. J., "Bond strength in concrete filled steel tubes", IABSE Proceedings, Vol. 33, 1980, pp 125–139.

[38] Lyu, W. Q. and Han L. H., "Investigation on bond strength between recycled aggregate concrete (RAC) and steel tube in RAC-filled steel tubes", Journal of Constructional Steel Research, Vol. 155, 2019, pp 438–459.

[39] De Oliveira, W. L. A., De Nardin, S., de Cresce El, A. L. H. and El Debs, M. K., "Influence of concrete strength and length/diameter on the axial capacity of CFT columns" Journal of Constructional Steel Research, Vol. 65, No. 12, 2009, pp 2103-2110.

[40] Lei, X., . Chengkui, H. and Yi, L., "Expansive performance of selfstressing and self-compacting concrete confined with steel tube", Journal of Wuhan University of Technology, Vol. 22, Februrary 2007, pp. 341-345.

[41] Xiong, M. X., Xiong, D. X., and Liew, J. Y. R., "Axial performance of short concrete filled steel tubes with high- and ultra-high-strength materials", Engineering Structure, Vol. 136, April 2017, pp 494–510.

[42] Xue, L. H., Cai, S. H., "Bond strength at the interface of concrete-filled steel tubular columns" Part I. Building Science, Vol. 12, No. 3, 1996, pp 22–28.

[43] Zhou, Z., Gan, D. and Zhou, X., "Improved composite effect of square concrete-filled steel tubes with diagonal binding ribs", Journal of Structural Engineering, ASCE, Vol. 145, No. 10, October 2019, pp 04019112: 1-12

[44] Zhu, J. Y., Chan, T. M. and Young, B., "Cross-sectional capacity of octagonal tubular steel stub columns under uniaxial compression" Engineering Structures, Vol. 184, 2019, pp 480-494.